MICRO-CHANNEL CONVECTIVE BOILING HEAT TRANSFER WITH FLOW INSTABILITIES

L. Consolini and J.R. Thome

Laboratoire de Transfert de Chaleur et de Masse, École Polytechnique Fédérale de Lausanne, Switzerland
lorenzo.consolini@epfl.ch, john.thome@epfl.ch

ABSTRACT

Flow boiling heat transfer in micro-channels has attracted much interest in the past decade, and is currently a strong candidate for high performance compact heat sinks, such as those required in electronics systems, automobile air conditioning units, micro-reactors, fuel cells, etc. Currently the literature presents numerous experimental studies on two-phase heat transfer in micro-channels, providing an extensive database that covers many different fluids and operating conditions. Among the noteworthy elements that have been reported in previous studies, is the sensitivity of micro-channel evaporators to oscillatory two-phase instabilities. These periodic fluctuations in flow and pressure drop either result from the presence of upstream compressibility, or are simply due to the interaction among parallel channels in multi-port systems. An oscillating flow presents singular characteristics that are expected to produce an effect on the local heat transfer mechanisms, and thus on the estimation of the two-phase heat transfer coefficients. The present investigation illustrates results for flow boiling of refrigerants R-134a, R-236fa, and R-245fa in a 510μm circular micro-channel, exposed to various degrees of oscillatory compressible volume instabilities. The data describe the main features of the fluctuations in the temperatures of the heated wall and fluid, and draw attention to the differences in the measured unstable time-averaged heat transfer coefficients with respect to those for stable flow boiling.

INTRODUCTION

Recent investigations on micro-channel flow boiling have pointed out the sensitivity of these small systems to oscillatory instabilities (see f. ex. [1-5]). In broad terms, the oscillations that have been reported refer to either (1) parallel channel instabilities, in the case of parallel channel evaporators with common inlet headers, or (2) to compressible volume instabilities, which may develop even in single-channel systems (see [6]). While parallel channel instabilities are essentially due to the interaction of the two-phase flow among adjacent channels, compressible volume instabilities may propagate in the presence of a degree of compressibility (a body of vapor, flexible hosing, etc.) upstream, or within, the heated length, and are the object of the present study. Although developed for sub-cooled flow boiling, the analysis of Maulbetsch and Griffith [7] offered very interesting insight into the phenomenon. To give a brief summary of their results, for the system depicted in Fig. 1, comprised of a heated length, an upstream buffer tank, an inlet pressure (p_{in}) that is function of the flow rate, and a constant exit pressure, oscillations in the mass flow and pressure drop were shown to propagate when the gradient of the pressure drop (Δp_1) versus flow curve (the internal characteristic, or "demand" curve, as shown in Fig. 2 for a two-phase flow) reached the critical value,

$$\left.\frac{d(\Delta p_1)}{dQ}\right|_{crit} = \frac{\frac{dp_{in}}{dQ}(I_1+I_2) + \sqrt{\left[\frac{dp_{in}}{dQ}(I_1+I_2)\right]^2 + 4I_1^2 I_2\left(\frac{dp}{dV}\right)_0}}{2I_2} \quad (1)$$

where Q is the total volumetric flow rate, and I_1 and I_2 are respectively the inertia of the flow in the heated section and of that into the buffer tank ($I = \rho L/A$, where ρ is the density of the flow, L is the length, and A is the cross-sectional area of the corresponding sector). The term $(dp/dV)_0$ is a measure of the compressibility within the buffer tank, into which mass accumulates before being sent periodically back to the heated test-section. In the two extreme cases of a constant flow delivery system and a constant pressure supply, the gradient to the external characteristic (the "supply" curve), dp_{in}/dQ, would yield: $dp_{in}/dQ \to -\infty$ and $dp_{in}/dQ = 0$ respectively. For the first case, a constant flow delivery system has the limits:

$$\left.\frac{d(\Delta p_1)}{dQ}\right|_{crit} = 0 \quad \text{and} \quad \omega^2 = \frac{\left(\frac{dp}{dV}\right)_0}{I_1 + I_2} \quad (2)$$

with ω the critical fluctuation frequency of both flow and pressure drop. This represents the least stable operating condition, since the oscillations would propagate as soon as the minimum is reached on the pressure drop-flow curve, as illustrated in Fig. 2. For the second case, the oscillatory

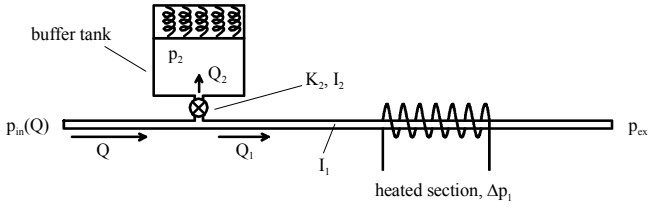

Figure 1. Schematic of the model for the analysis of oscillatory instabilities, where subscript 1 refers to the flow through the heated length, while subscript 2 refers to the flow into the compressible volume.

instability is not expected to occur, since only a rise in the inlet pressure could induce a flow into the compressible volume. As implied by Eq. (2), the critical frequency of an unstable flow will depend on the system and on the available compressibility. Kenning and Yan [8] reported oscillations in local pressure and wall temperature for experiments with different degrees of inlet compressibility. Their power spectrum analysis on both pressure and temperature signals gave peak values at frequencies around 6Hz. Brutin *et al.* [9] reported a stability diagram for their experiments on n-pentane flowing in a single rectangular channel with a hydraulic diameter $D_h = 889\mu m$. Their experimental setup was similar to that in Fig. 1, but with a vertical heated section, and from their flow visualizations, they observed the instability and associated it to significant oscillations in pressure drop at around 4Hz. On the other hand, frequencies as low as 0.2Hz were reported by Wang *et al.* [10] for their tests in the presence of parallel channel instabilities.

As the oscillation in the flow takes place, the evaporator experiences a cyclical boiling behavior, which, in the most general case, may be described as the periodic development of five distinct stages (see [11]): (1) single-phase liquid filling of the channel, (2) bubble nucleation over the channel length, (3) growth and coalescence of bubbles to form a vapor pouch over almost the entire cross-section, (4) a rapid expansion of the vapor that may involve the entire channel length, and (5) evaporation of the quasi-static liquid film left at the channel wall after the bubble expansion. The bubble in stage (4) may induce blockage of the flow in the heated section, or, if it grows towards the inlet, will provoke backflow of liquid into an upstream compressible volume or into adjacent channels.

Oscillations in pressure drop, flow, and wall temperatures are the typical symptoms of these instabilities, and are often found in the micro-channel literature. The periodic development of substantial dry-zones, along with possible fluctuations in the saturation temperature (coupled to the propagation of pressure pulses in the fluid), may explain the wall temperature oscillations. In [11] and [12] it was shown that for sufficiently high heat fluxes the liquid film left by the expanding bubble may dry-out, thus leaving the channel wall periodically in contact with only vapor. At medium heat fluxes bubble nucleation may have a stronger impact on heat transfer than the convective boiling process induced by the bubble expansion. The five-part sequence essentially reduces to the growth of the bubbles at the wall followed by liquid refilling of the channel, yielding heat transfer coefficients that are independent of vapor quality and that present the typical nucleate boiling characteristics. At higher heat fluxes and lower mass velocities, the onset of nucleation shifts towards the channel inlet, and substantial convective vaporization results from the rapid bubble expansions. The probability of dry-out of the liquid film increases in the flow direction, and may explain some of the reported decreasing heat transfer coefficients with increasing vapor quality. This was also suggested in the study of Agostini and Bontemps [13]. Nonetheless, film dry-out may or may not occur depending on the value of the applied heat flux. The observations in [8], for example, involved only back and forward oscillations of elongated bubbles; thus less severe excursions are also possible.

Among the studies that illustrated local heat transfer coefficients, computed from time-averaged wall and fluid temperatures, in the presence of oscillatory instabilities, Xu *et al.* [11] (flow boiling of acetone in 10 triangular channel with $D_h = 155\mu m$) argued that the extent of these flow oscillations determined different behaviors in the heat transfer coefficient, and associated each to an interval in the Boiling number ($Bo \equiv q/(Gh_{lv})$). Hetsroni *et al.* [12] reported data for water in a 21 parallel triangular micro-channel evaporator, and a single rectangular channel with $D_h = 590\mu m$. The data from [12] show very high values for the heat transfer coefficient at low vapor qualities that decrease rapidly with x. Cortina Díaz and Schmidt [14] tested water and ethanol in a singular rectangular channel with $D_h = 590\mu m$. In their study, the authors described the periodic temperature oscillations in their heated wall (5Hz for ethanol while no characteristic frequency was observed for water). As in [12], their computed heat transfer coefficients for water showed very high peaks at low vapor qualities, decreasing dramatically with $x = 0.2$.

The objective of the present investigation is to further study the characteristics of micro-channel flow boiling affected by a compressible volume instability. Experimental results are illustrated for flow boiling of refrigerants R-134a, R-236fa, and R-245fa in a 510μm circular micro-channel, exposed to various degrees of oscillation. The data describe the main features of the fluctuations in the temperatures of the heated wall and of the fluid, and draw attention to the differences in the measured local heat transfer coefficients with respect to those for stable flow boiling.

EXPERIMENTAL FACILITY

The experimental test stand is illustrated in Fig. 3, and includes two pressurized vessels, a Coriolis Mass Flowmeter (CMF), a flow adjustment valve and the test-section. All tubing, other than for the test-section, is 4mm in internal diameter. The flow is driven by the pressure difference between the two vessels, each of which contains saturated liquid and vapor of the refrigerant. The vessels are thus maintained at different pressures/temperatures by means of external thermal regulating units. This setup avoids having to use components with moving parts, i.e. a pump, which may induce undesirable vibrations. Saturated liquid, extracted from the bottom of the high pressure tank, crosses the CMF, enters the test-section through the valve, and is then directed into the

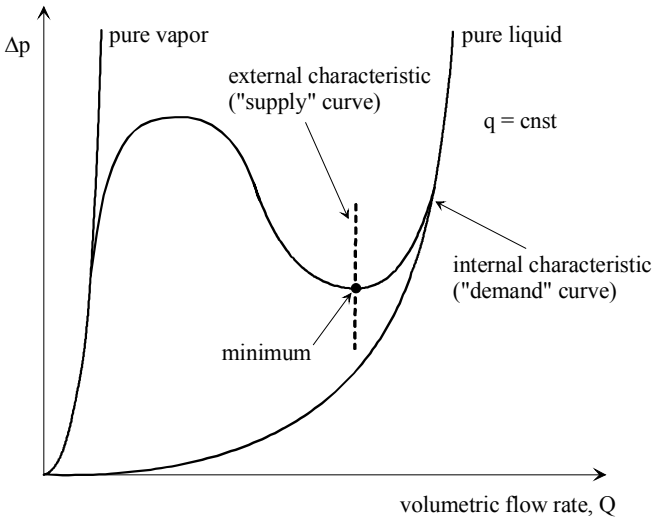

Figure 2. The internal and external characteristic curves for an evaporating flow at constant heat flux. The external characteristic is representative of a constant flow delivery system.

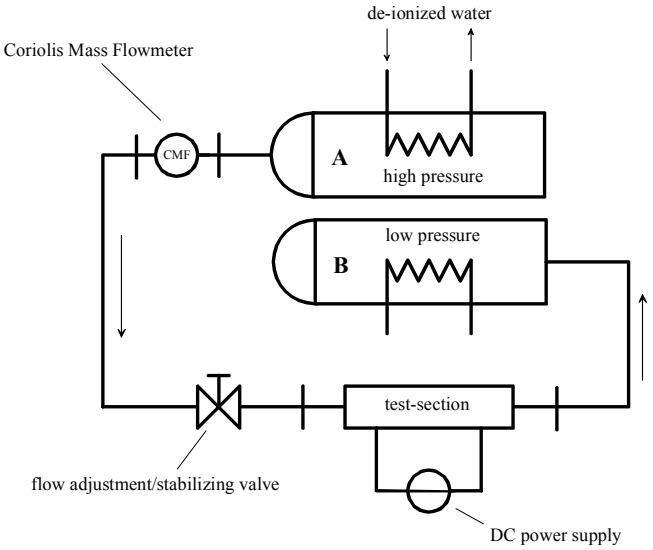

Figure 3. A diagram of the experimental facility.

low pressure vessel.

The test-section, illustrated in Fig. 4, includes the circular micro-channel (D = 510μm), all the connections to the electric power supply units, and the instrumentation required for the measurements. The three main sectors to the test-section are (1) the pre-heater, for setting the desired inlet conditions to the evaporator, (2) the evaporator, where boiling occurs and heat transfer is measured, and (3) the glass tube for flow visualization. All three channels have the same sizes, and the junctions between each sector are manufactured to allow for precise alignment. Both the pre-heater and evaporator are made from stainless steel, and each has a pair of copper electrodes to electrically heat the channel and thus the flow (by DC current). Two pressure taps are located immediately upstream and downstream of the test-section, while type K thermocouples (50μm leads) are positioned on the outer walls of both pre-heater and evaporator. The thermocouple leads are placed within individual support shells to avoid breakage, and the hot junctions are pressed against the tube wall through external springs thus reducing contact resistance. A fine layer of insulating varnish is placed between the junction and the tube wall to avoid electrical disturbance.

Inlet and outlet fluid temperatures are obtained from wall temperature measurements taken at the two adiabatic locations before and after the heated lengths (EV_{in} and EV_{out} in Fig. 4). The other thermocouples, positioned on the heated length (between the electrodes), provide the outer temperatures of the wall that are then used to evaluate the local heat transfer coefficients (inner wall temperatures are back-calculated from the measured values). The two pairs of electrodes (pre-heater and evaporator) are connected to two separate DC power supplies. The intensity of the applied current is measured by a current intensity meter, while the voltage drop is measured directly at the electrodes.

An upstream compressible volume results from a mild degree of flashing of the saturated liquid extracted from the high-pressure vessel. The small amount of vapor produced through the pressure reduction process is trapped at the top of a cylindrical sight glass positioned prior to the CMF. Flow stability is regulated by the valve at the entrance to the test-section (see Figs. 3 and 5), which "isolates" the boiling flow in the evaporator from the upstream compressibility. As the valve is opened, while maintaining fixed operating conditions by adjusting the pressures in the two vessels, the resistance to any backflow is reduced. If the conditions are such that the pressure pulse from the bubble formation process is strong enough, an oscillatory instability will propagate, with liquid being cyclically injected into the compressible volume.

DATA REDUCTION

For a complete description of the data reduction scheme refer to [15]. Local heat transfer coefficients are evaluated at every temperature measurement point on the heated length of the evaporator. The heat transfer coefficient, α, is defined in terms of the magnitude of the inner wall heat flux (q), and the difference between the inner wall temperature (T_w) and that of the bulk fluid (T_f):

$$\alpha \equiv \frac{q}{T_w - T_f} \tag{3}$$

The temperature of the inner wall is derived from the time-averaged value of the measured outer wall temperature by a one-dimension heat conduction calculation with internal heat generation,

$$T_w = T_1 + \frac{q'''_g D_1^2}{k_w}\left[1 - \left(\frac{D}{D_1}\right)^2 + 2\ln\left(\frac{D}{D_1}\right)\right] \tag{4}$$

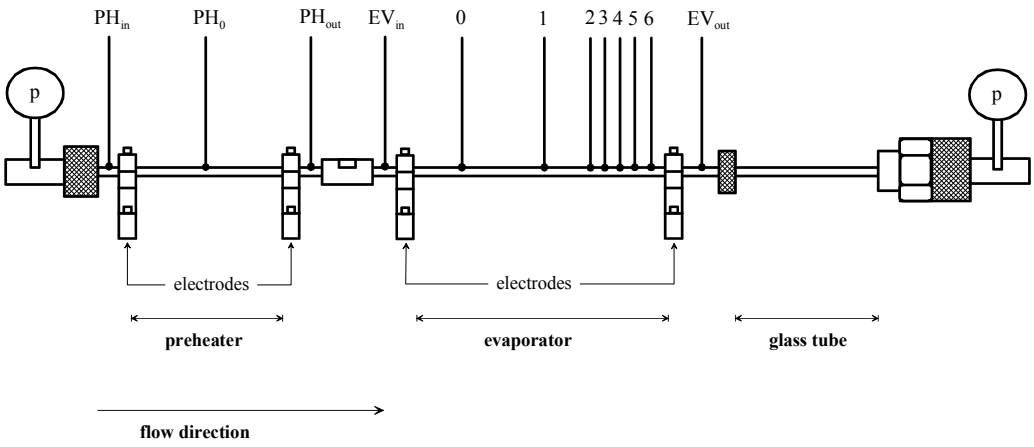

Figure 4. Schematic diagram of the flow boiling test-section showing the two pressure taps (p) at the inlet and exit, and the locations of the pre-heater (PH) and evaporator (EV) thermocouples.

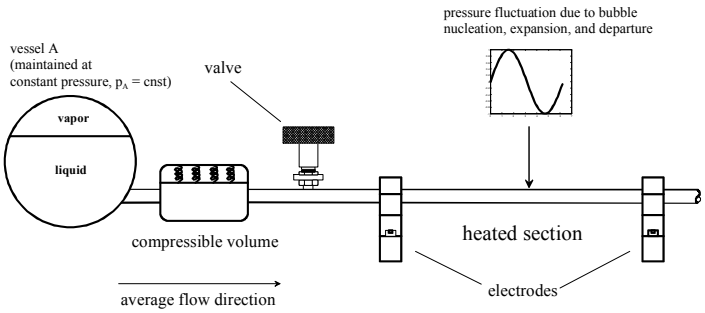

Figure 5. Schematic showing the test-section, the valve, and the upstream compressible volume, as occurs in the present test facility.

where T_1 is the temperature of the outer wall, D_1 and D are respectively the outer and inner diameters of the tube, and k_w is the wall material thermal conductivity. The heat generation term in Eq. (4) is evaluated from the measured current (I) and voltage drop (ΔV) across the stainless steel evaporator as

$$q'''_g = \frac{4\eta I \Delta V}{\pi (D_1^2 - D^2) L} \tag{5}$$

The heating efficiency, η, in Eq. (5) is assessed by computing the heat losses by conduction and natural convection from the test-section, verified by single-phase tests. The wall heat flux is then determined assuming a uniform distribution as,

$$q = \frac{\eta I \Delta V}{\pi D L} \tag{6}$$

The fluid temperature in Eq. (3) corresponds to the saturation temperature of the fluid and is computed assuming a linear pressure drop over the saturated length, utilizing the time-averaged pressure values at the inlet and outlet to the evaporator.

Local vapor qualities are evaluated from the specific enthalpy of the liquid phase (h_l) and the latent heat of vaporization (h_{lv}), both taken at the local pressure, and the specific enthalpy of the flow (h),

$$x = \frac{h - h_l}{h_{lv}} \tag{7}$$

with h given as,

$$h(z) = \frac{4q}{GD} z + h_0 \tag{8}$$

where G is the total mass flux, z is the local axial coordinate and h_0 is the inlet ($z = 0$) enthalpy.

RESULTS AND DISCUSSION

Temperature fluctuations

Figure 6 illustrates a comparison of a "stable" temporal profile for the outer wall temperature, with the fluctuations generally within the uncertainty band of the thermocouples, to

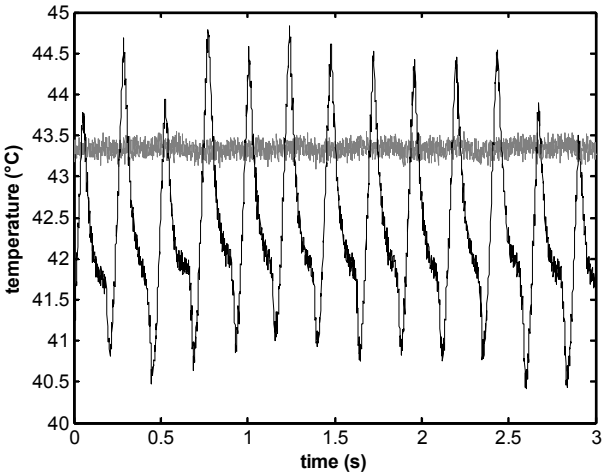

Figure 6. Steady outer wall temperature during flow boiling, (shown in gray) and wall temperature during flow instability (black curve). Values refer to R-245fa in the 510μm tube, a heat flux of 50kW/m^2, and mass velocities of 500kg/m^{2}s (steady case) and 400kg/m^{2}s (unstable case).

that of an unstable flow. As mentioned previously, the instability onset is obtained by gradually opening the valve at entrance to the test-section, while adjusting the system parameters in order to maintain fixed conditions in the evaporator. As shown in Fig. 6 for the unstable flow, the temperature fluctuation with respect to the mean is about ±2.0°C, much lower than the ±0.15°C of the stable flow. Furthermore, the temperature cycle is quite repeatable in both shape and magnitude, with a frequency of about 4Hz.

The amplitude of the oscillation increases when increasing heat flux while maintaining its periodicity. Figure 7 illustrates the change in the measured wall temperature for an unstable flow of R-236fa with varying heat flux. Higher heating also changes the shape of the curves. Figure 8 shows a set of results for R-245fa. For the temperatures of the heated wall (left column in Fig. 8), the low heat flux case presents two main oscillation modes at 4.4 and 7.3Hz. As the heat flux is increased, the second mode dampens, and eventually disappears entirely at 87kW/m^2.

Recalling the description given in the Introduction, the

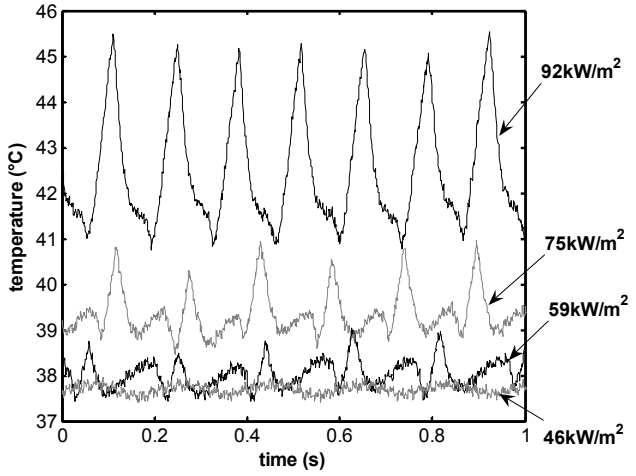

Figure 7. Wall temperature fluctuations taken 65mm downstream of the entrance to the evaporator, for an R-236fa at 31°C flowing with a mass velocity of 700kg/m^{2}s.

periodic wall temperatures are essentially due to (1) the local change in flow temperature associated to the pressure fluctuations due to the bubble growth, expansion, and flushing process, and (2) the cyclical variations in the heat transfer mechanisms. Figure 8 shows the oscillations in the temperature of the fluid exiting the evaporator, at different levels of heat flux. The temperature at the lowest heat flux presents one main mode at 4.4Hz, which is also found in the wall temperature. However, there is no presence of the second mode at 7.3Hz, which may indicate that although the change in fluid temperature contributes to the behavior of the wall temperature, the fluctuations in the local heat transfer coefficient (pure convection of liquid, thin film evaporation in the films surrounding elongated bubbles, and convective vaporization in the annular film), also play an important role. This appears even clearer at the highest heat flux, where the

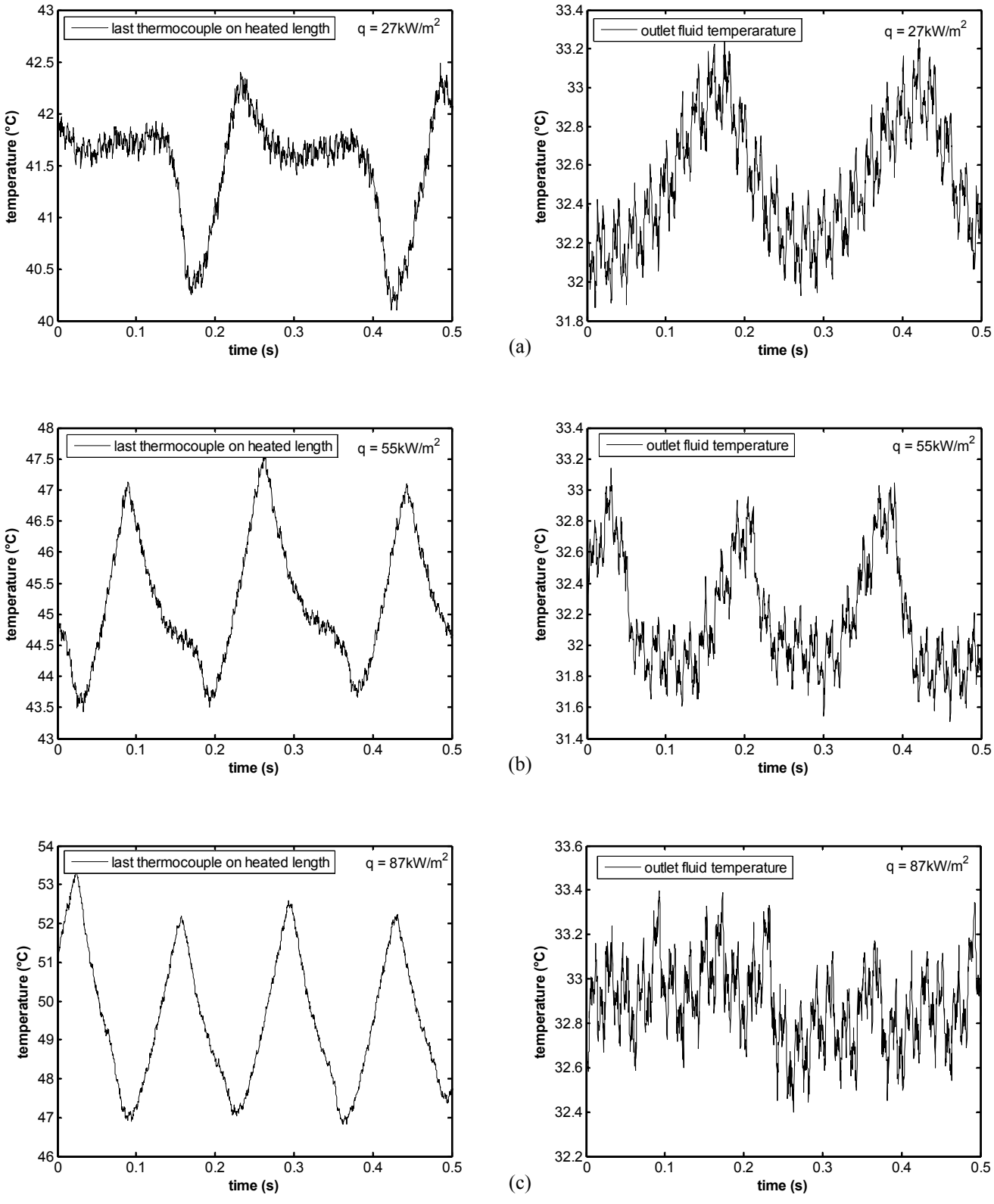

Figure 8. Fluctuations in the wall and fluid temperatures for unstable flow boiling of R-245fa, with a mass velocity of 400kg/m^{2}s, and at heat fluxes of (a) 27, (b) 55, and (c) 87kW/m^2 (510μm tube).

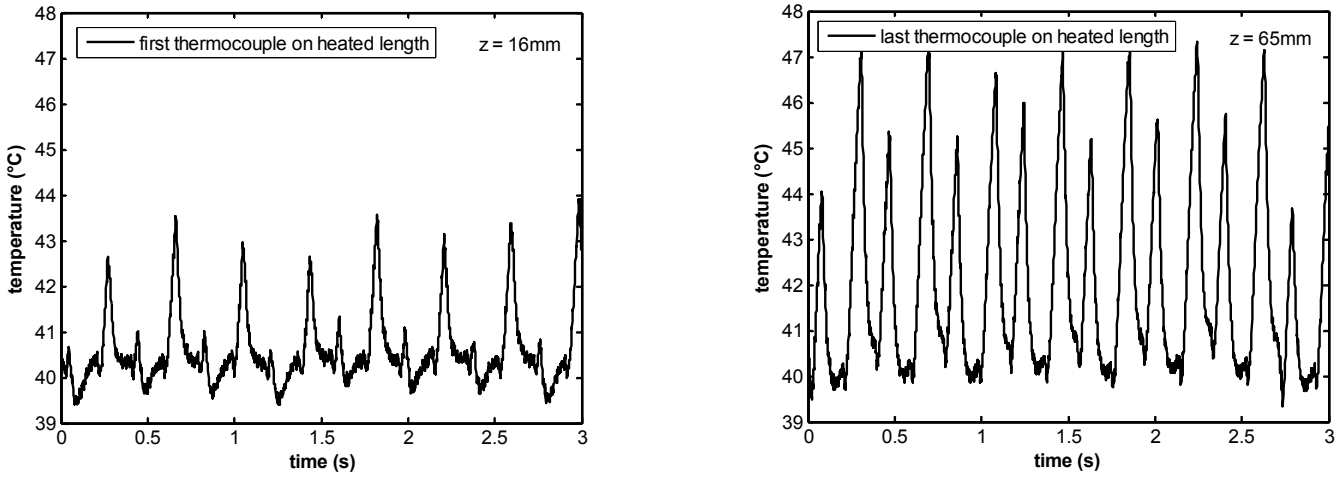

Figure 9. Wall temperature fluctuations from the first and last thermocouples (19 and 65mm from the inlet respectively) on the heated length, for unstable flow boiling of R-236fa at a heat flux of 87kW/m^2 and an average mass velocity of 400kg/m^{2}s.

oscillation in the fluid temperature is extremely irregular, while the wall temperature fluctuates vigorously (note that the wall temperature plots in Fig. 8 refer to the thermocouple closest to the exit).

The features of the temperature oscillations are also affected by the axial measurement location. Figure 9 shows the temperatures from the first and last thermocouples on the heated length for a flow of R-236fa. The amplitude of the temperature fluctuation of the first thermocouple is lower with respect to the one further downstream. While the last temperature on the heated length has one main oscillation mode at 5.4Hz, the first presents two frequencies: a main one at 2.4Hz and a secondary mode at 7.8Hz.

As a final note, of the three fluids considered for the current study, R-245fa, the lowest pressure fluid, exhibits the highest sensitivity to the instability, which is most likely due to the following reasons: (1) the vapor phase of R-245fa presents the highest compressibility/lowest stiffness (the vapor stiffness of R-245fa at 30°C, here defined as $(\partial p/\partial v)_T = -\rho^2(\partial p/\partial \rho)_T$, is lower than that of R-134a by a factor of 20), and (2) R-245fa presents the highest two-phase pressure drop (R-245fa combines a high liquid viscosity with a low vapor density, relative to the other two fluids), thus its internal characteristic is shifted upward in the pressure drop versus flow rate plane, yielding a higher value for the critical flow rate.

Two-phase heat transfer coefficients

In order to assess the differences in the estimated heat transfer coefficients between a stable and an unstable flow, several tests were performed under unstable conditions. Figure 10 compares corresponding heat transfer measurements for four sets of data: one refers to a stable flow of R-245fa, while the remaining three refer to flows exposed to instabilities of different degrees. The data for the unstable cases are computed utilizing time-averaged wall and fluid temperatures (over a 3s period and a sampling rate of 1000 samples per second). For the run with mild oscillations (a maximum amplitude in the outer wall temperature of $\Delta T_1 \approx 0.5$°C), the heat transfer coefficients behave as in the case of a stable flow. However, once the flow becomes notably unstable, the outer wall temperature fluctuations reach amplitudes of $\Delta T_1 \approx 4$°C, and their mean values change, delivering completely different trends in the α-x plane. Fig. 10 shows an absolute deviation from the stable flow data of 42% at a vapor quality of $x = 0.26$. For the data in Fig. 10, the uncertainty on the heat transfer coefficients increases from ±6% for the stable experiments to ±24% for the unstable measurements. Although the largest effect of instability in the heat transfer coefficients occurs for R-245fa, R-236fa also exhibits similar differences with respect to equivalent stable flow boiling. On the other hand, R-134a requires a very high heat flux for the instabilities to propagate.

The heat transfer data for flows affected by the oscillatory phenomenon generally show minimal influence of mass velocity, with slightly downward trends with vapor quality in the α-x plane (Figs. 11 and 12), as was previously noticed in the investigations by Xu *et al.* [11] and Hetsroni *et al.* [12]. The coefficients were often seen to increase with heat flux, although not in all cases, as shown in Fig. 13. From some of the data, it appears that for sufficiently high heat fluxes, the heat transfer coefficients become less sensitive to q, and may at times decrease with higher heating levels. The present results show quite conclusively that published data must be segregated into stable and unstable categories in order to be useful for development of prediction methods.

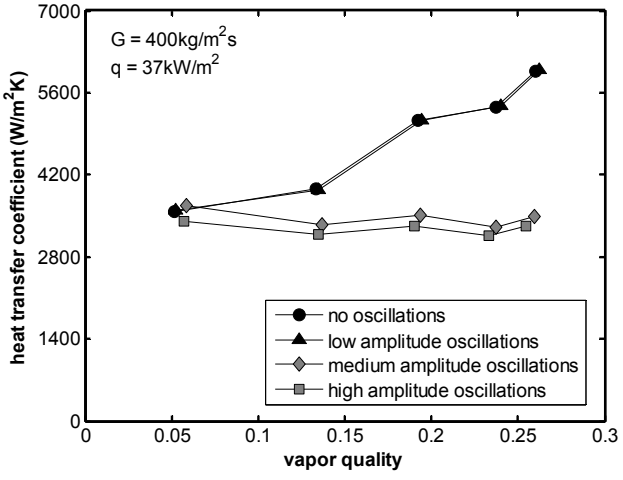

Figure 10. Stable and unstable heat transfer coefficients for R-245fa with $D = 510\mu$m, $T_{in} = 30$°C and $T_{out} = 32$°C

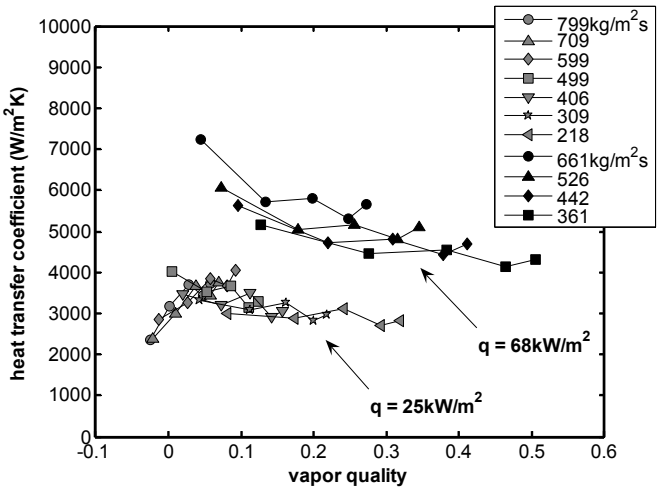

Figure 11. Heat transfer coefficients computed from unstable flow data for R-245fa at 32°C, at two levels of heat flux and a range of mass velocities.

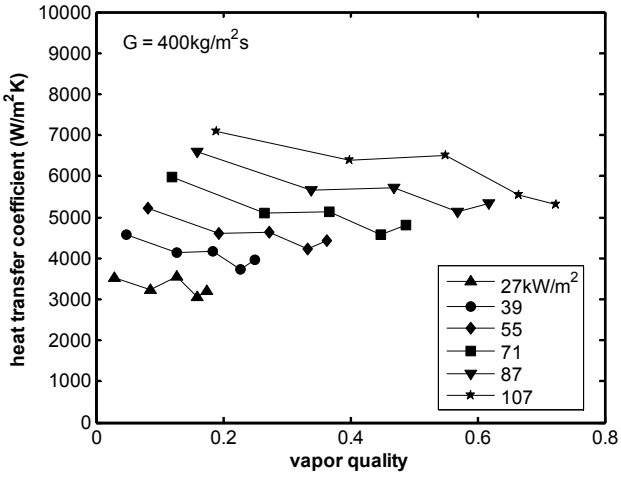

Figure 12. Heat transfer coefficients computed from unstable flow data for a R-245a at 33°C flowing at 400kg/m^{2}s.

CONCLUSIONS

A flow affected by a compressible volume instability is exposed to oscillations in the local pressure and temperature and in the heat transfer mechanisms. The global effect on the heated wall is a corresponding temperature oscillation, which combines both of these effects. Assessing local heat transfer coefficients from a flow that is subjected to instability, neglecting the fluctuations, may lead to a substantial deviation from a corresponding stable flow. It is therefore of paramount importance to distinguish between stable and oscillating two-phase flows in the measurement of flow boiling heat transfer coefficients in micro-channels, in order to avoid superposing data of two different natures in the development and validation of two-phase heat transfer models and correlations.

NOMENCLATURE

Latin

A	cross-sectional area	m^2
Bo	boiling number, $q/(Gh_{lv})$	-
D	diameter	m
G	mass velocity	kg/m^{2}s
h	specific enthalpy	J/kg
I	inertia	kg/m^4
k	thermal conductivity	W/mK
L	tube length	m
p	pressure	Pa
Q	volumetric flow rate	m^3/s
q	heat flux	W/m^2
T	temperature	°C
V	volume	m^3
v	specific volume	m^3/kg
x	vapor quality	-
z	axial coordinate	m

Greek

α	heat transfer coefficient	W/m^{2}K
η	heating efficiency	-
ω	oscillation frequency	rad/s
ρ	density	kg/m^3

Subscripts

crit	critical
g	heat generation

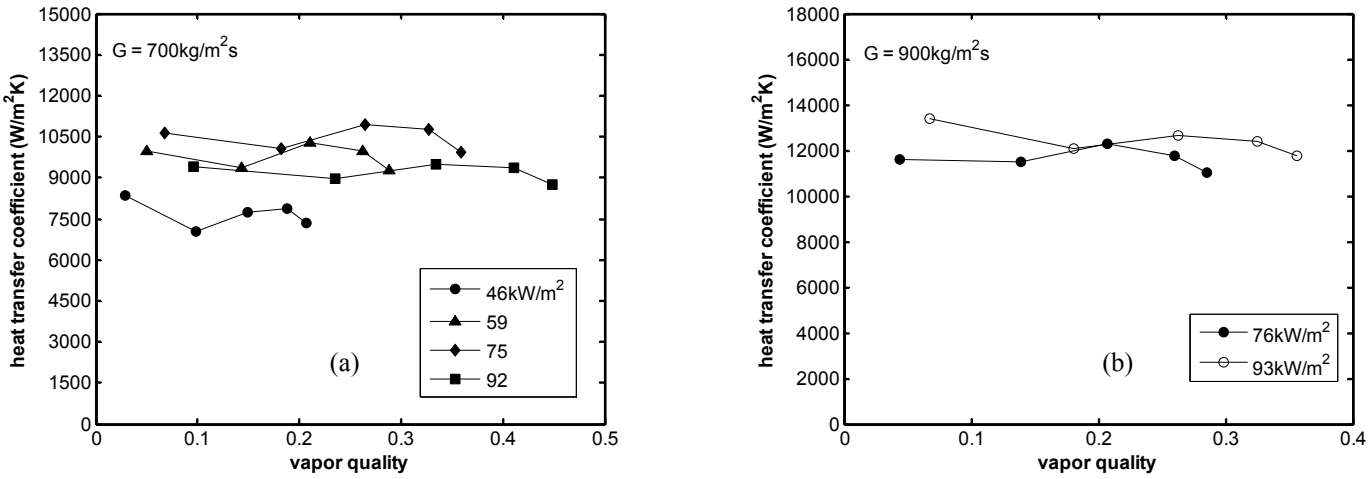

Figure 13. Heat transfer coefficients computed from unstable flow data of R-236fa at 31°C with (a) G = 700kg/m^{2}s and (b) G = 900kg/m^{2}s, and different heat fluxes.

h	hydraulic
in	inlet
l	liquid
lv	liquid-vapor
out	outlet
w	wall

0	inlet enthalpy
1	referring to the outer diameter

REFERENCES

1. W. Qu and I. Mudawar, Measurement and Prediction of Pressure Drop in Two-Phase Micro-Channel Heat Sinks, *Int. J. Heat Mass Transfer*, vol. 46, pp. 2737-2753, 2003.
2. P. Balasubramanian and S.G. Kandlikar, Experimental Study of Flow Patterns, Pressure Drop and Flow Instabilities in Parallel Rectangular Minichannels, *Heat Transfer Engineering*, vol. 26, pp. 20-27, 2005.
3. C. Huh, J. Kim and M.H. Kim, Flow Pattern Transition Instability During Flow Boiling in a Single Microchannel, *Int. J. Heat Mass Transfer*, vol. 50, pp. 1049-1060, 2007.
4. K.H. Chang and C. Pan, Two-Phase Flow Instability for Boiling in a Microchannel Heat Sink, *Int. J. Heat Mass Transfer*, vol. 50, pp. 2078-2088, 2007.
5. S.L. Qi, P. Zhang, R.Z. Wang and L.X. Xu, Flow Boiling of Liquid Nitrogen in Micro-Tubes: Part I – The Onset of Nucleate Boiling, Two-Phase Flow Instability and Two-Phase Flow Pressure Drop, *Int. J. Heat Mass Transfer*, vol. 50, pp. 4999-5016, 2007.
6. A.E. Bergles and S.G. Kandlikar, On the Nature of Critical Heat Flux in Microchannels, *J. Heat Transfer*, vol. 127, pp. 101-107, 2005.
7. J.S. Maulbetsch and P. Griffith, A Study of System-Induced Instabilities in Forced-Convection Flows with Subcooled Boiling, Air Force Contract AF 49(638)-1468, Report No. 5382-35, April 1965.
8. D.B.R. Kenning and Y. Yan, Saturated Flow Boiling of Water in a Narrow Channel: Experimental Investigation of Local Phenomena, *Trans IChem*, vol. 79, part A, pp. 425-436, 2001.
9. D. Brutin, F. Topin, and L. Tadrist, Experimental Study of Unsteady Convective Boiling in Heated Minichannels, *Int. J. Heat Mass Transfer*, vol. 46, pp. 2957-2965, 2003.
10. G. Wang, P. Cheng and A.E. Bergles, Effects of Inlet/Outlet Configurations on Flow Boiling Instability in Parallel Microchannels, *Int. J. Heat Mass Trasnsfer*, vol. 51, pp. 2267-2281, 2008.
11. J. Xu, S. Shen, Y. Gan, Y. Li, W. Zhang and Q. Su, Transient Flow Pattern Based Microscale Boiling Heat Transfer Mechanisms, *J. Micromech. Microeng.*, vol. 15, pp. 1344-1361, 2005.
12. G. Hetsroni, A. Mosyak, E. Pogrebnyak, and Z. Segal, Explosive Boiling of Water in Parallel Micro-Channels, *Int. J. Multiphase Flow*, vol. 31, pp. 371-392, 2005.
13. B. Agostini, and A. Bontemps, Vertical Flow Boiling of Refrigerant R134a in Small Channels, *Int. J. Heat and Fluid Flow*, vol. 26, pp. 296-306, 2005.
14. M. Cortina Díaz and J. Schmidt, Experimental Investigation of Transient Boiling Heat Transfer in Micro-Channels, *Int. J. Heat Fluid Flow*, vol. 28, pp. 95-102, 2007.
15. L. Consolini, Convective Boiling Heat Transfer in a Single Micro-Channel, Ph.D. thesis, École Polytechnique Fédérale de Lausanne, Lausanne, Switzerland, 2008. Available at: http://library.epfl.ch/theses/?nr=4024.